Sensitivity of DRAKKAR global simulations to two existing and a hybrid atmospheric forcing functions

Thierry Penduff, Bernard Barnier, Laurent Brodeau, Mélanie Juza

Sensitivity of DRAKKAR global simulations to two existing and a hybrid atmospheric forcing functions

Thierry PENDUFF
Bernard BARNIER
Laurent BRODEAU
Mélanie JUZA

DRAKKAR : LEGI (Grenoble), LPO (Brest), LODYC (Paris), LEGOS (Toulouse), LSCE (Gif-sur-Yvette), IFM-GEOMAR (Kiel, Germany), Shirshov Institute of Oceanology (Moscow, Russia), Helsinki University (Finland).

LEGI, Grenoble, France

DRAKKAR

Main objective :
Study the ocean variability and scale interactions since 1950
Hierarchy of numerical models :
Global ocean (horizontal resolutions: 2°, 1/2°, 1/4°)
North Atlantic/Nordic Seas basin (1/4°, 1/12°)
NEMO system(5) : OPA9-LIM
explicit simulation of the 3-dimensional ocean circulation, sea-ice, 14C and CFC tracers.
Surface forcing :
momentum, heat and water fluxes computed online via bulk formulae from prognostic model SSTs and atmospheric variables (wind, temperature, specific humidity).
Among other OST/ST objectives :
improve the surface forcing of high-resolution ocean models by hybridizing reanalyzed fields with satellite products.
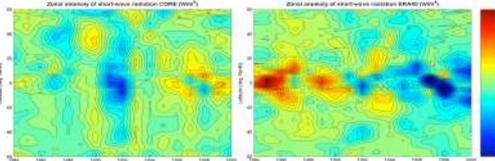
3 STEPS

1. Prior to ocean simulations and given a reference time/space-dependent SST dataset, a **stand-alone tool named FOTO** is first used to estimate the impact of various forcing functions (bulk formulations, atmospheric variables) on air-sea fluxes and on large-scale integrated balances.
2. **Coarse-resolution (2° resolution) global simulations** are then performed, driven by these forcing functions. This second step extends the former results by representing the feedback of large-scale ocean dynamics on SST and air-sea interactions (e.g. advection/subduction of forced buoyancy anomalies).
3. Both steps should eventually help investigate the impact of the surface forcing in **50-year full-resolution (1/4° to 1/12°) simulations**, in which additional degrees of freedom related to the ocean mesoscale are at work.

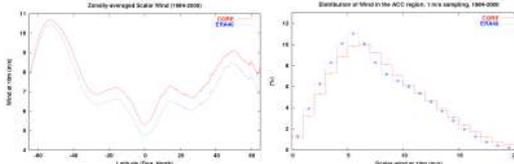The first two steps of this approach are illustrated in this study.

3 FORCING FIELDS

The air-sea fluxes and the oceanic response to **CORE**(1) and **ERA40**(2) surface forcing functions are compared via FOTO and from the 2° global simulations. A third forcing function has been constructed by **hybridizing long- and short-wave downwelling radiation fields from the ISCCP satellite-derived dataset into the ERA40 function**.


Input Variables

Variable	Name	CORE	ERA40	HYB
Wind (10m)	Ua,Va	NCEP/NCAR (corr.)	ECMWF	ECMWF
Air temp. (10m)	Ta	NCEP/NCAR (corr.)	ECMWF	ECMWF
Air hum. (10m)	qa	NCEP/NCAR (corr.)	ECMWF	ECMWF
Radiation	Qsw,Qlw	ISCCP-FP (satellite)	ECMWF	ISCCP-FP (satellite)
Precipitation	P	GPCP, Xie & Arkin	ECMWF	ECMWF

Stronger zonally-averaged scalar winds in CORE. High winds are more frequent in ERA40 than in CORE, while moderate winds blow less often.

Disagreement between CORE and ERA40 on the time variability of the zonally-averaged solar radiative flux (Qsw). ERA40 exhibits a negative trend at low latitudes.
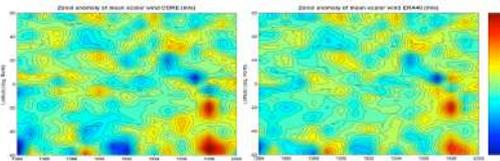
Good agreement between CORE and ERA40 on the variability of the zonally-averaged wind at 10m (|Ua|).

Differences between CORE and ERA40 are mainly found on solar radiation (Qsw) and surface winds, two variables of major importance for forcing the ocean. With turbulent fluxes varying non-linearly with wind speeds, it is important to investigate the wind speed distribution in key regions. Solar radiation is the only source of heat for the ocean and its steady decrease at low latitudes in ERA40 is expected to adversely affect the simulations.

Despite a very similar time variability, CORE winds are stronger than ERA40 at every latitude. CORE forcing is thus more likely to enhance heat loss by evaporation and to lead to a stronger surface circulation.

FOTO : Fluxes from observed SST

Forcing functions
$$\vec{U}_a \; , \; T_a \; , \; q_a$$
$$q_{sw}^{sky} \; , \; q_{lw}^{sky}$$
$$P \; , \; R$$

SST (obs. or model prognostic)

Bulk formulae
$$Q_{net} = Q_{sw} + Q_{lw} + Q_{lat} + Q_{sen}$$
$$Q_{sw} = (1 - \alpha_s) q_{sw}^{sky}$$
$$Q_{lw} = q_{lw}^{sky} - \varepsilon_o \sigma SST^4$$
$$Q_{sen} = \rho_a C_p C_H (T_a - SST) |\vec{U}_a|$$
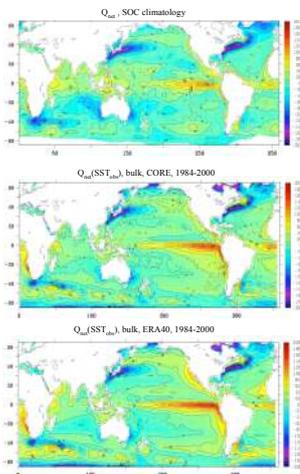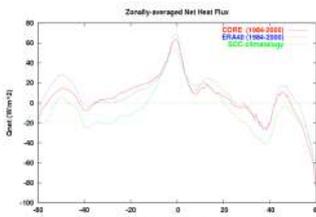$$E = \rho_a C_E (q_a - q_{sat}(SST)) |\vec{U}_a|$$
$$Q_{lat} = L_{vap} E$$
$$\vec{\tau} = \rho_o C_D |\vec{U}_a - \vec{U}_s| \vec{U}_a$$

Air-sea fluxes
• Q_{net}
• $\vec{\tau}$
• $P + R - E$

OCEAN MODEL

Air-sea fluxes are computed online through bulk formulae during the model integrations, and depend on prognostic SSTs. The resulting fluxes are then applied at the ocean surface. This loop mimics the feedback between the lower atmosphere and the upper ocean, and adds degrees of freedom to the system.

Prior to model integrations, the FOTO tool is used to compare the air-sea fluxes derived from available *forcing functions* and observed SST fields (Hurrell, 3). These fluxes are compared to the SOC (4) flux climatology.

This procedure shows that for a given SST, ERA40 injects more heat into the ocean at almost every latitude (except at mid southern).


Model simulations at 2° resolution
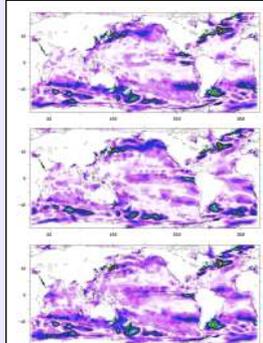
The 2° global ocean/seaice DRAKKAR model has been forced over 17 years (1984-2000) by **CORE**, **ERA40** and **HYB**. HYB is ERA40 using the same radiative product as CORE.
Figures to the left show the RMS difference between monthly-averaged model SSTs and the Hurrell(3) climatology over 17 years. The modeled sea-ice concentrations are compared over 1990-2000 to a SSM/I ice product(6) in the southern hemisphere. Figures below present the global imbalance for each run over the same period.
The **CORE** run predicts a better SST, except at mid southern latitudes (45-25°S) where **ERA40** is better by almost 0.5°C. In the same region **HYB** sticks to CORE, showing that the solar radiation is responsible for this trend. In all runs the maximum discrepancies happen along the eddy-active extensions of the Gulfstream and the Kuroshio.
All 3 runs show a net trend to heat storage, but HYB has the lowest inbalance over the 17 years.
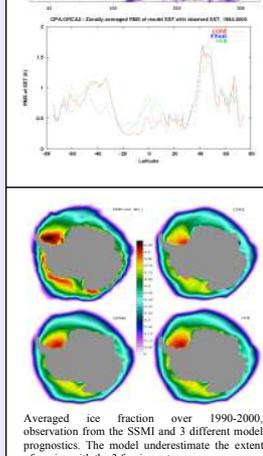
Averaged ice fraction over 1990-2000, observation from the SSMI and 3 different model prognostics. The model underestimate the extent of sea ice with the 3 forcing sets.
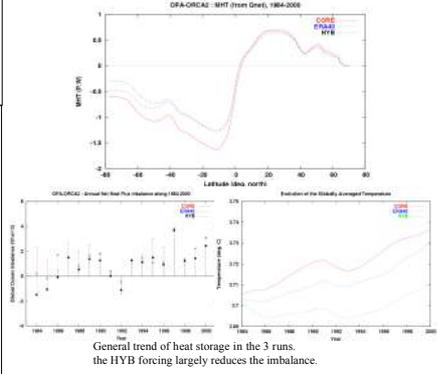
General trend of heat storage in the 3 runs. the HYB forcing largely reduces the imbalance.

CONCLUSION

Neither CORE nor ERA40 clearly appear as the ocean modeler's best choice. The preliminary analysis of input variables and the offline test reveal noticeable differences between both datasets, but model outputs are rather close to each other. CORE leads to the most realistic results, but leads to a warming trend. The new HYB combination of ERA40 with the radiative product of CORE removes this large net heat flux imbalance while preserving CORE's qualities. These coarse-resolution results will be extended at high resolution (1/4°) to reveal the contribution of eddy and non-linear processes.

REFERENCES

(1) Large, W. G. and Yeager, S. G. 2004, *Diurnal to Decadal Global Forcing For Ocean and Sea-Ice Models: The Data Sets and Flux Climatologies.* NCAR technical note, 62 pp.
(2) European Centre for Medium-Range Weather Forecasts, 2002: The ERA-40 Archive. ECMWF, 40 pp.
(3) Hurrell, J., Caron, J., Hack, J. & Shea, D. 2003, *A New Surface Temperature and Sea Ice boundary data set for the Community Atmosphere Model*, Geophys. Res. Lett. pp. 0-999.
(4) Josey, S., Kent, C. and Taylor, P. 1998, *The Southampton Oceanography Centre (SOC) ocean-atmosphere heat, momentum and freshwater flux atlas*, Technical Report No. 6, Southampton Oceanography Centre, 30pp.
(5) Madec, G., P. Delecluse, M. Imbard, and C. Lévy, 1998: OPA 8.1 Ocean General Circulation Model reference manual. Note du Pôle de modélisation, Institut Pierre-Simon Laplace, N°11, 91pp.
(6) Comiso, J. 1999, Bootstrap Sea Ice Concentrations for NIMBUS-7 SMMR and DMSP SSM/I, Digital Media, National Snow and Ice Data Center.